Optical Study of Archetypical Valence-Fluctuating Eu Systems

V. Guritanu,[1] S. Seiro,[1] J. Sichelschmidt,[1] N. Caroca-Canales,[1] T. Iizuka,[2] S. Kimura,[2] C. Geibel,[1] and F. Steglich[1]

[1]*Max Planck Institute for Chemical Physics of Solids, 01187 Dresden, Germany*
[2]*UVSOR Facility, Institute for Molecular Science, Okazaki 444-8585, Japan*

(Received 6 June 2012; published 12 December 2012)

We have investigated the optical conductivity of the prominent valence-fluctuating compounds $EuIr_2Si_2$ and $EuNi_2P_2$ in the infrared energy range to get new insights into the electronic properties of valence-fluctuating systems. For both compounds, we observe upon cooling the formation of a renormalized Drude response, a partial suppression of the optical conductivity below 100 meV, and the appearance of a midinfrared peak at 0.15 eV for $EuIr_2Si_2$ and 0.13 eV for $EuNi_2P_2$. Most remarkably, our results show a strong similarity with the optical spectra reported for many Ce- or Yb-based heavy-fermion metals and intermediate valence systems, although the phase diagrams and the temperature dependence of the valence differ strongly between Eu systems and Ce- or Yb-based systems. This suggests that the hybridization between $4f$ and conduction electrons, which is responsible for the properties of Ce and Yb systems, plays an important role in valence-fluctuating Eu systems.

DOI: 10.1103/PhysRevLett.109.247207 PACS numbers: 75.20.Hr, 71.27.+a, 75.30.Mb, 78.20.−e

Intermetallic compounds based on rare-earth elements with an unstable valence, especially Ce, Eu, and Yb, present many unusual properties and therefore have been the subject of intense research for many years. Historically, the understanding of these compounds has been dominated by a dichotomy between the Kondo-lattice (KL) or intermediate-valence (IV) scenario for Ce- or Yb-based systems and the valence-fluctuating (VF) scenario for Eu-based systems. The former scenario considers a quantum mixing of two valence states induced by the hybridization V_{fc} between localized f electrons and conduction electrons. In contrast, the latter scenario corresponds to a thermal fluctuation between two integer-valence states. The best criterion to differentiate between these two cases is the evolution of the valence ν as a function of temperature T and composition x or pressure p. In KL or IV systems, increasing the hybridization leads to a smooth and continuous evolution of ν as a function of p or x. As a result, the magnetic order observed for small V_{fc} disappears smoothly and the ordering temperature T_N continuously decreases to zero at a quantum critical point [Fig. 1(a)] [1]. Even beyond the quantum critical point the change of ν as a function of temperature is small, usually less than 0.1 between 0 and 300 K. VF Eu systems instead present a pronounced first-order valence transition as a function of p or x from a divalent Eu state with a large-moment magnetic order to an almost trivalent state showing Van Vleck paramagnetism [Fig. 1(b)] [2,3]. For $p > p_c$ or $x > x_c$, one observes a first-order valence transition line, which ends at a critical end point at finite temperature. Well beyond the critical end point the change of ν in Eu systems is typically still larger than 0.5 between 0 and 300 K.

The nature of the electronic states and the low-energy excitations in Ce- or Yb-based KL or IV systems have been studied in great detail by optical spectroscopy [4–8] and are relatively well understood. However, for Eu-based VF systems, this knowledge is very limited and no optical studies have yet been published. Recent developments have challenged the KL or VF dichotomy, suggesting that valence fluctuations are strongly relevant for classical heavy-fermion systems [9]. For instance, valence fluctuations are suspected to induce the superconductivity dome found at high pressure in $CeCu_2Si_2$ [10–12]. Therefore, getting a deeper understanding of VF systems and their electronic structure has become an important issue.

In this Letter, we present a study of the electrodynamic response of two prominent VF Eu systems, $EuIr_2Si_2$ and $EuNi_2P_2$. Our results reveal an optical conductivity that is surprisingly similar to that of KL or IV systems: upon decreasing temperature we observe in both Eu compounds the formation of a renormalized Drude response, a partial suppression of the optical conductivity, and a well-defined mid-infrared (MIR) peak at about 150 meV. This is in strong contrast to the huge difference in the temperature dependence of the valence between Ce- or Yb-based KL or IV systems and Eu-based VF systems.

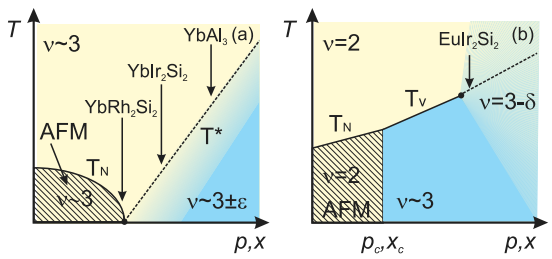

FIG. 1 (color online). Schematic phase diagrams of (a) KL or IV Ce-($\nu \sim 3 + \epsilon$) or Yb-($\nu \sim 3 - \epsilon$) based systems and (b) VF Eu-based systems; [$\epsilon, \delta = f(x, p, T)$].

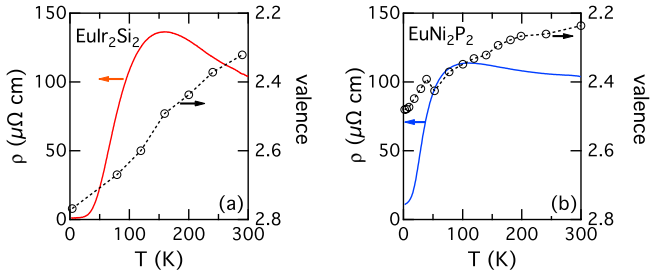

FIG. 2 (color online). Resistivity and valence as a function of temperature of $EuIr_2Si_2$ and $EuNi_2P_2$. The valence data are taken from Refs. [13,14].

$EuIr_2Si_2$ is an archetypical VF Eu system with a valence deduced from Mössbauer experiments [13] that decreases from 2.8 at 4 K to 2.3 at 300 K [Fig. 2(a)]. $EuNi_2P_2$ presents a unique situation among Eu-based VF systems. At high temperatures ($T > 100$ K), it is similar to $EuIr_2Si_2$, but at low temperature its valence [14], instead of approaching 3, remains close to 2.5; see Fig. 2(b). The reason $EuNi_2P_2$ at low temperatures differs from standard VF Eu systems such as $EuCu_2Si_2$, $EuNi_2Si_2$, or $EuIr_2Si_2$ is presently not clear. As shown in Fig. 2, the resistivity $\rho(T)$ of $EuIr_2Si_2$ ($EuNi_2P_2$) increases upon cooling below 300 K and passes through a broad maximum at about 150 K (100 K) before decreasing dramatically towards low temperatures. This temperature dependence reflects the valence fluctuations [15] but also looks quite similar to that observed for Yb- or Ce-based IV systems. For both materials at low temperatures, below 20 K, the resistivity and specific heat show a Fermi-liquid behavior.

Single crystals of $EuIr_2Si_2$ and $EuNi_2P_2$ were synthesized as described in Refs. [3,16]. Near-normal incidence reflectivity spectra were measured using a Fourier transform spectrometer Bruker IFS 66 v/S at energies 10 meV–0.8 eV in the temperature range from 6 to 260 K. To obtain the absolute value of the reflectivity, a gold layer was evaporated *in situ* on the crystal surface. At room temperature the reflectivity was measured for energies 0.6–1.25 eV using a Jasco FTIR 610 spectrometer, where an Al mirror was used as a reference, and from 1.2 to 30 eV using synchrotron radiation at the beam line 7B of UVSOR-II, Institute for Molecular Science. For $EuIr_2Si_2$, the reflectivity measurements were extended down to 4 meV using a Jasco FARIS-1 spectrometer.

Figures 3(a) and 3(b) display the infrared reflectivity spectra $R(\omega)$ of $EuIr_2Si_2$ and $EuNi_2P_2$ for various temperatures down to 6 K. The general shape of $R(\omega)$ and the trend of changes are very similar for both materials, indicating a resemblance of their electrodynamic properties. At low energy, $R(\omega)$ increases with decreasing temperature and approaches unity when $\omega \rightarrow 0$ as expected for a metal. On the other hand, in the energy range between 30 and 200 meV, $R(\omega)$ is strongly suppressed, and a dip structure develops upon cooling, which is more pronounced for $EuIr_2Si_2$. This suppression in the reflectivity spectra at low temperatures signals the development of a pseudogap. Interestingly, as shown in the insets of Figs. 3(a) and 3(b) the temperature dependence of the spectra becomes stronger below 200 K (100 K) for $EuIr_2Si_2$ ($EuNi_2P_2$) where the resistivity also shows a sharp decrease. Besides these features, for $EuIr_2Si_2$ a

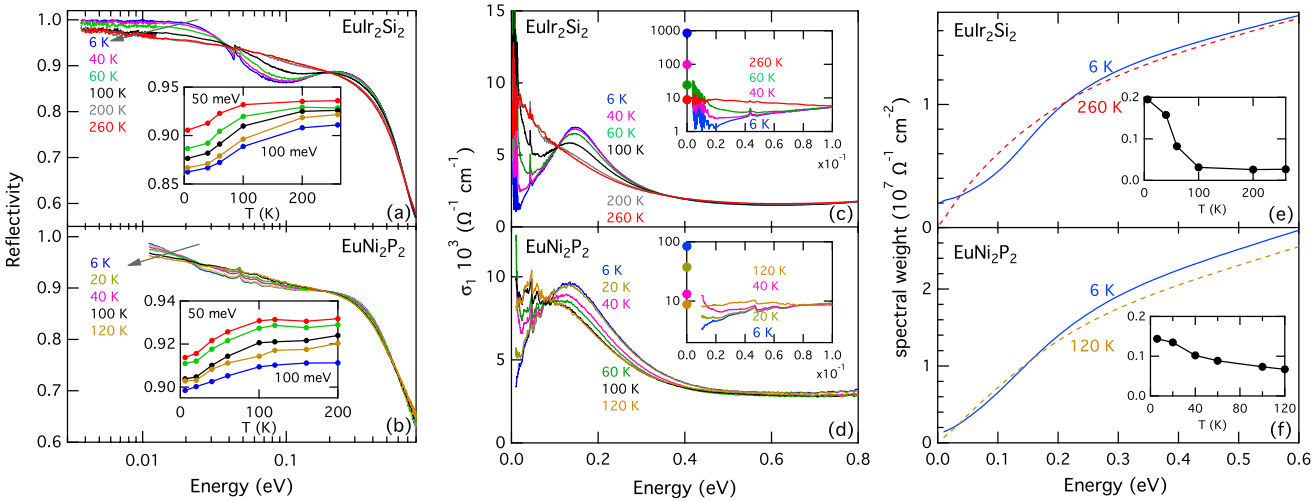

FIG. 3 (color online). [(a) and (b)] Reflectivity spectra of $EuIr_2Si_2$ and $EuNi_2P_2$ at various temperatures. For $EuIr_2Si_2$, the sharp peak at 44 meV is an infrared active phonon mode. The structure seen at 47 meV in the spectra of both materials is an experimental artifact. Insets: Temperature dependence of $R(\omega)$ at 50, 60, 68, 80, and 100 meV (from top to bottom). [(c) and (d)] Real part of the optical conductivity spectra of $EuIr_2Si_2$ and $EuNi_2P_2$ at various temperatures. Insets: Low-energy optical conductivity spectra (solid lines) and the corresponding values for the dc conductivity $\sigma_{dc} = \rho^{-1}$ (circles) at 6, 40, 60, and 260 K for $EuIr_2Si_2$ and at 6, 20, 40, and 120 K for $EuNi_2P_2$. [(e) and (f)] Partial spectral weight $\int_0^{\omega} \sigma_1(\omega')d\omega'$ at 6 and 260 K (6 and 120 K) for $EuIr_2Si_2$ ($EuNi_2P_2$). Insets: Temperature dependence of the spectral weight at the lowest measured energy.

sharp peak due to an infrared active phonon emerges at 44 meV.

The optical conductivity was derived from the measured reflectivity spectra in combination with the independently measured dc conductivity data using a Kramers-Kronig consistent variational fitting procedure [17]. Figures 3(c) and 3(d) show the real part of the optical conductivity spectra $\sigma_1(\omega)$ of $EuIr_2Si_2$ and $EuNi_2P_2$. As the temperature is lowered, three remarkable structures emerge in the optical conductivity of both materials. First, at the lowest measured energies, an intraband response of heavy quasiparticles is indicated by tails of narrow Drude-like peaks. This is implied for both materials by the behavior of the dc conductivities σ_{dc} and the low-energy optical data as shown in the insets of Figs. 3(c) and 3(d): between high and low temperatures, σ_{dc} increases by a factor of 100 (10) for $EuIr_2Si_2$ ($EuNi_2P_2$). Second, the optical conductivity strongly decreases below 100 meV with decreasing temperature. This leads to a depletion of the spectral weight immediately above the narrow Drude-like peak indicating the opening of a pseudogap. The third feature is the MIR peak centered at 0.15 eV for $EuIr_2Si_2$ and at 0.13 eV for $EuNi_2P_2$. The peak maximum is slightly shifted toward lower energy with increasing temperature and vanishes above ≈ 100 K.

In VF systems, it seems natural to relate the MIR peak to the energy difference between the divalent and the trivalent configurations. However, using the phenomenological model of interconfiguration fluctuations [18] to fit the susceptibility $\chi(T)$ or the valence $\nu(T)$ results in an energy difference of about 200 K. This is an order of magnitude smaller than the energy of the MIR peak ($\equiv 1600$ K). In the Falicov-Kimball (FK) model [19], which is the basic Hamiltonian describing the VF systems, the distinctive ingredient is the on-site Coulomb repulsion U_{fc} between an f electron and a conduction electron. This model predicts a MIR peak located at U_{fc}, while the valence transition occurs at a temperature much lower in comparison to that of U_{fc}. The energy of the MIR peak is an order of magnitude larger than the temperature of the maxima in $\rho(T)$ (see Fig. 2) or $\chi(T)$, in qualitative agreement with the FK model. However, this model predicts a decrease of the intensity of the MIR peak with decreasing temperature, while the experiment [Figs. 3(c) and 3(d)] shows an increase of its intensity upon cooling, in strong disagreement with the calculations. As suggested in Ref. [19], this might be related to the absence of any hybridization term in the FK model. It is worth mentioning that the FK model predicts an isosbestic point for the optical conductivity [20], which is indeed observed at around 100 meV for both compounds; see Figs. 3(c) and 3(d).

The optical conductivities and their temperature dependence that we observed in VF Eu systems are very similar to the typical features reported for Ce- or Yb-based KL or IV systems [4–8]. This is quite remarkable since the characteristic phase diagrams and the temperature evolution of the valence are very different for VF Eu systems and Ce- or Yb-based KL or IV systems [3]. Therefore, one would expect the optical spectra and their energy and temperature dependence to be very different, too. In the Ce- or Yb-based KL or IV systems, the formation of a narrow Drude peak, a pseudogap, and a MIR peak are attributed to the hybridization between localized f electrons and conduction electrons [5]. Thus, the optical data for $EuIr_2Si_2$ and $EuNi_2P_2$ strongly indicate that the hybridization between $4f$ and conduction electrons plays an important role in understanding the low-energy optical spectra of VF Eu compounds. This is supported by recent angle-resolved photoemission measurements on $EuNi_2P_2$ where localized $4f$ states were observed to hybridize with valence states as in Ce- or Yb-based KL systems, resulting in $4f$ dispersion and the opening of hybridization gaps [16].

The optical spectral weight is temperature dependent, as shown in Figs. 3(e) and 3(f). It is redistributed around the isosbestic points, but a transfer towards higher energies also seems to be realized. The latter is most obviously seen for $EuNi_2P_2$, where the missing spectral weight is clearly not fully recovered at 0.6 eV. This indicates that strong electronic correlations dominate the charge dynamics at low energies. Moreover, as shown in the insets of Figs. 3(e) and 3(f), the spectral weight at the lowest measured energies reveals a clear temperature dependence also indicating a temperature dependence of the Drude weight. This implies that the electronic structure of both Eu systems is changing at low temperature and supports our statement on the relevance of hybridization in VF Eu systems. To further analyze the temperature and energy evolution of the low-energy excitations, we plot in Figs. 4(a)–4(d) the energy dependence of the scattering rate $\tau^{-1}(\omega)$ and the effective mass $m^*(\omega)$ relative to the band mass m obtained from an extended Drude analysis [21],

$$\frac{1}{\tau(\omega)} = \frac{\omega_p^2}{4\pi}\mathrm{Re}\left[\frac{1}{\sigma(\omega)}\right], \qquad \frac{m^*(\omega)}{m} = \frac{\omega_p^2}{4\pi\omega}\mathrm{Im}\left[\frac{1}{\sigma(\omega)}\right].$$

Here, one should note that this model is meaningful in the energy range below the interband transitions, where the optical conductivity is dominated by the response of mobile carriers. We assume that at energies lower than 100 meV the contribution of interband transitions to the optical conductivity is negligible and this model can be applied. Therefore, we determined the plasma frequencies $\omega_p = 3$ eV (3.9 eV) through $m^*/m = 1$ at $\omega = 80$ meV for $EuIr_2Si_2$ ($EuNi_2P_2$). It should be mentioned that the magnitude of m^*/m depends on the chosen values for ω_p, but the general shape is unaffected. Our choice of ω_p leads to reasonable values of the optical resistivity $\rho_{opt}(\omega) = \mathrm{Re}[1/\sigma(\omega)] = 4\pi/[\tau(\omega \to 0)\omega_p^2]$, in good agreement with the measured dc data. For both materials, we observe at low temperature strong energy- and temperature-dependent effective masses and scattering rates, indicating

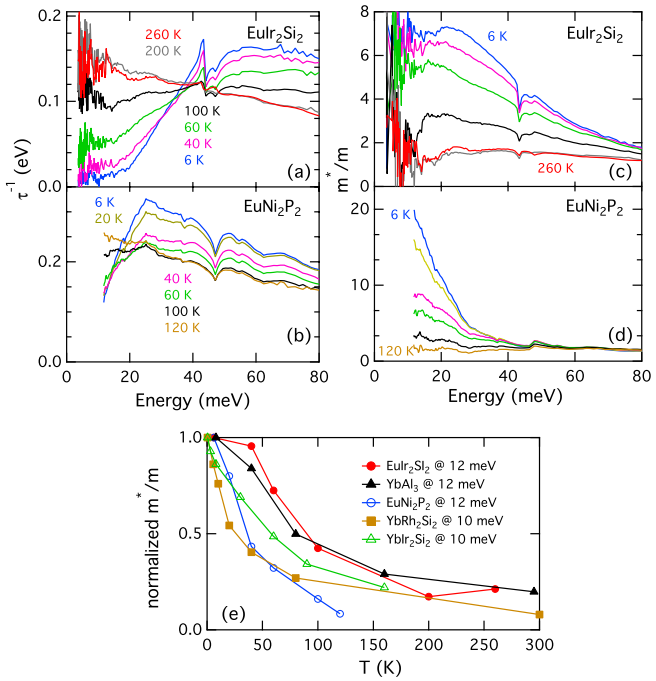

FIG. 4 (color online). [(a) and (b)] Scattering rate and [(c) and (d)] effective mass relative to band mass as a function of energy for $EuIr_2Si_2$ and $EuNi_2P_2$. (e) Normalized effective mass for $EuIr_2Si_2$ and $EuNi_2P_2$. As a comparison, the data for $YbIr_2Si_2$ [6], $YbRh_2Si_2$ [7], and $YbAl_3$ [8] are shown.

deviations from the simple Drude response. The data reveal that the energy and temperature scales are larger for $EuIr_2Si_2$. At 6 K and the lowest measured energy, we find $m^*/m \sim 8$ (20) for $EuIr_2Si_2$ ($EuNi_2P_2$). These values are in good agreement with results of specific heat measurements, where the ratio of the Sommerfeld coefficient of $EuIr_2Si_2$ ($EuNi_2P_2$) to that of its noncorrelated homolog $LaIr_2Si_2$ ($LaNi_2P_2$) amounts to 7.3 (17.5) [3,22]. Such a moderate mass enhancement is comparable to values reported for Ce- or Yb-based IV compounds with a similar characteristic $4f$ energy.

Notwithstanding the optical similarities to the KL or IV systems, specific differences regarding the effective mass of VF Eu systems can be identified. In Fig. 4(e), we compare the temperature evolution of the effective masses normalized to their low-temperature values for $EuIr_2Si_2$ and $EuNi_2P_2$ with the data for the heavy-fermion metals $YbIr_2Si_2$ [6] and $YbRh_2Si_2$ [7] as well as the IV compound $YbAl_3$ [8]. A closer look at the normalized m^*/m values reveals characteristic differences, which can be linked to the different natures of each compound. For $YbRh_2Si_2$, $YbIr_2Si_2$, and $EuNi_2P_2$, the effective mass drops rapidly upon increasing temperature. In contrast, in the archetypical VF Eu system $EuIr_2Si_2$, the effective mass remains almost constant up to 40 K where a steep drop sets in. The low-temperature behavior in the IV system $YbAl_3$ is in between, with some evidence for a negative curvature around 40 K.

A further difference becomes obvious when the absolute values of m^*/m are considered. The mass renormalization around 100 K is still quite large in $YbRh_2Si_2$ and $YbIr_2Si_2$ ($m^*/m \sim 50$) [6,7] and in $YbAl_3$ ($m^*/m \sim 15$) [8] while in $EuIr_2Si_2$ and $EuNi_2P_2$ no significant enhancement is observed ($m^*/m \sim 3$). A similar difference is also observed in the temperature dependence of the MIR peak, which disappears above 100 K in the VF Eu systems but is still clearly visible at 300 K in $YbAl_3$. This is in line with expectations from the underlying models. The Anderson model [23], being based on hybridization effects with conduction electrons, results in a logarithmic temperature dependence at high temperatures, which implies some renormalization up to very high temperatures. In contrast, for VF systems close to the first-order valence transition such as $EuIr_2Si_2$, the FK model predicts strong changes in a narrow temperature range. However, the differences between our results on the VF Eu systems and those reported for Ce- or Yb-based KL or IV systems are much less pronounced than one might have expected from these models.

In conclusion, we have studied the optical properties in the infrared energy range of the prominent VF systems $EuIr_2Si_2$ and $EuNi_2P_2$. For both materials, we observe upon decreasing temperature the formation of a narrow Drude-like response, a partial suppression of the optical conductivity below 100 meV, and a MIR peak at 0.15 eV for $EuIr_2Si_2$ and 0.13 eV for $EuNi_2P_2$. These results present striking similarities to those reported for Ce- or Yb-based KL or IV systems, despite the much stronger change of the valence as a function of temperature and a completely different phase diagram as a function of pressure or chemical tuning in VF Eu systems. Our analysis highlights the importance of hybridization between f and conduction electrons in the VF Eu systems. Our results call for further theoretical calculations of the optical properties for the extended periodic Anderson model Hamiltonian combining a hybridization term with an intrasite Coulomb repulsion between f and conduction electrons [10,24,25].

We thank Dr. A. Irizawa for kindly sharing his beam time at UVSOR. We also acknowledge S. Kostmann and K. Imura for technical assistance and H. Okamura for sharing his optical data for $YbAl_3$. V. G. benefited from financial support from the Alexander von Humboldt Foundation.

[1] Q. Si and F. Steglich, Science **329**, 1161 (2010).
[2] C. U. Segre, M. Croft, J. A. Hodges, V. Murgai, L. C. Gupta, and R. D. Parks, Phys. Rev. Lett. **49**, 1947 (1982).
[3] S. Seiro and C. Geibel, J. Phys. Condens. Matter **23**, 375601 (2011).
[4] S. R. Garner, J. N. Hancock, Y. W. Rodriguez, Z. Schlesinger, B. Bucher, Z. Fisk, and J. L. Sarrao, Phys. Rev. B **62**, R4778 (2000).
[5] F. P. Mena, D. van der Marel, and J. L. Sarrao, Phys. Rev. B **72**, 045119 (2005).

[6] T. Iizuka, S. Kimura, A. Herzog, J. Sichelschmidt, C. Krellner, C. Geibel, and F. Steglich, J. Phys. Soc. Jpn. **79**, 123 703 (2010).
[7] S. Kimura, J. Sichelschmidt, J. Ferstl, C. Krellner, C. Geibel, and F. Steglich, Phys. Rev. B **74**, 132408 (2006).
[8] H. Okamura, T. Michizawa, T. Nanba, and T. Ebihara, J. Phys. Soc. Jpn. **73**, 2045 (2004).
[9] S. Watanabe and K. Miyake, J. Phys. Condens. Matter **24**, 294 208 (2012).
[10] Y. Onishi and K. Miyake, J. Phys. Soc. Jpn. **69**, 3955 (2000).
[11] H. Q. Yuan, F. M. Grosche, M. Deppe, C. Geibel, G. Sparn, and F. Steglich, Science **302**, 2104 (2003).
[12] A. T. Holmes, D. Jaccard, and K. Miyake, Phys. Rev. B **69**, 024508, (2004).
[13] B. Chevalier, J. M. D. Coey, B. Lloret, and J. Etourneau, J. Phys. C **19**, 4521 (1986).
[14] R. Nagarajan, G. K. Shenoy, L. C. Gupta, and E. V. Sampathkumaran, J. Magn. Magn. Mater. **47–48**, 413 (1985).
[15] E. Zipper, M. Drzazga, and A. Freimuth, J. Magn. Magn. Mater. **71**, 119 (1987).
[16] S. Danzenbächer *et al.*, Phys. Rev. Lett. **102**, 026403 (2009).
[17] A. B. Kuzmenko, Rev. Sci. Instrum. **76**, 083108 (2005).
[18] B. C. Sales and D. K. Wohlleben, Phys. Rev. Lett. **35**, 1240 (1975).
[19] V. Zlatić and J. K. Freericks, Acta Phys. Pol. B **32**, 3253 (2001).
[20] J. K. Freericks and V. Zlatić, Rev. Mod. Phys. **75**, 1333 (2003).
[21] A. V. Puchkov, D. N. Basov, and T. Timusk, J. Phys. Condens. Matter **8**, 10 049 (1996).
[22] R. A. Fisher, P. Radhakrishna, N. E. Phillips, J. V. Badding, and A. M. Stacy, Phys. Rev. B **52**, 13 519 (1995); R. J. Goetsch, V. K. Anand, A. Pandey, and D. C. Johnston, Phys. Rev. B **85**, 054517 (2012); H. F. Braun, T. Jarlborg, and A. Junod, Physica (Amsterdam) **135B**, 397 (1985).
[23] A. C. Hewson, *The Kondo Problem to Heavy Fermions* (Cambridge University Press, Cambridge, England, 1993).
[24] Y. Saiga, T. Sugibayashi, and D. S. Hirashima, J. Phys. Soc. Jpn. **77**, 114 710 (2008).
[25] K. Kubo, J. Phys. Soc. Jpn. **80**, 114 711 (2011).